Spectral identification of diffuse resonances in H2 above the n=2 dissociation limit

Ivanov, T.I.; de Lange, C.A.; Ubachs, W.M.G.

published in
Journal of Chemical Physics
2011

DOI (link to publisher)
10.1063/1.3544300

document version
Publisher's PDF, also known as Version of record

Spectral identification of diffuse resonances in H_2 above the $n = 2$ dissociation limit

T. I. Ivanov, C. A. de Lange, and W. Ubachs[a)]
Institute for Lasers, Life and BioPhotonics, VU University, De Boelelaan 1081, 1081 HV Amsterdam, The Netherlands

(Received 20 November 2010; accepted 3 January 2011; published online 3 February 2011)

The resonance structure in molecular hydrogen above the $n = 2$ dissociation limit is experimentally investigated in a 1 XUV + 1 VIS coherent two-step laser excitation process, with subsequent ionization of H($n = 2$) products. Diffuse spectral features exhibiting widths of several cm^{-1} in the excitation range of 118 500–120 500 cm^{-1} are probed. Information on angular momentum selection rules for parallel and crossed polarizations, combination differences, the para–ortho distinction, extrapolation from rovibrational structure in the bound region below the $n = 2$ threshold, and mass-selective detection of H_2^+ parent and H^+ daughter fragments is used as input. This allows for an assignment of the diffuse resonances observed in terms of $^1\Sigma_g^+$, $^1\Pi_g$, and $^1\Delta_g$ states, specified with vibrational and rotational quantum numbers. © *2011 American Institute of Physics*. [doi:10.1063/1.3544300]

I. INTRODUCTION

The quantum level structure of the smallest molecule and the benchmark system of molecular physics, H_2, can be conveniently subdivided into compartments. The quantum states of *triplet* symmetry have been investigated over many decades; we refer to the metastable $c^3\Pi_u$, $v = 0$ state discovered by Lichten,[1] later used to perform high-resolution laser spectroscopic studies,[2] and the studies on dissociation in the triplet manifold.[3,4] The spin–orbit interaction between levels of *singlet* and *triplet* symmetry is very small, to the extent that for a long time the separation between singlet and triplet quantum levels was erroneously deduced.[5] In this investigation on the level structure of singlet symmetries in H_2 the effect of the triplet states can be safely ignored.

A second distinction can be made between quantum states of *gerade* and of *ungerade* inversion symmetry. Even in the case of breakdown of the Born–Oppenheimer approximation, there is no interaction between states belonging to these subclasses, while at the same time one-photon optical transitions occur only between states of u and g characters. The states of singlet-u symmetry have been investigated via the strong dipole-allowed $B^1\Sigma_u^+ - X^1\Sigma_g^+$ Lyman and $C^1\Pi_u - X^1\Sigma_g^+$ Werner bands at high accuracy in the laboratory and at high redshift in quasars.[6,7] The next higher lying $D^1\Pi_u$ system (pre)-dissociates above the $n = 2$ limit; the dissociation is caused by coupling to continua associated with bound states below $n = 2$, most notably of the $B'^1\Sigma_u^+$ continuum.[8,9] In the singlet-u compartment there is no repulsive state causing the dissociation, in contrast to the situation in the singlet-g compartment.

The excited states in the singlet-g compartment of H_2 cannot be reached in single–photon excitation from the $X^1\Sigma_g^+$ ground state. Over many decades the level energies of $^1\Sigma_g^+$, $^1\Pi_g$, and $^1\Delta_g$ states were investigated in spectroscopic emission studies in the optical domain, with a wealth of data laid down in the *Dieke atlas*.[10] Further, series of *gerade* states, some of high angular momentum ($4f$, $5g$, and $6h$), were observed in Fourier-transform emission studies by Herzberg, Jungen and co-workers.[11–13] Later, multiphoton excitation was used in particular to investigate $EF^1\Sigma_g^+$, the lowest excited state in this compartment.[14,15] Tsukiyama and coworkers performed fluorescence lifetime measurements on a variety of singlet-g quantum levels in H_2 below the $n = 2$ dissociation limit,[16,17] and in addition some metastable levels of (f)-symmetry for the various hydrogen isotopomers.[18] The level structure of singlet-g states was unraveled based on nonadiabatic *ab initio* calculations in the comprehensive work by Yu and Dressler.[19] Ross and Jungen succeeded in providing assignments of the bound *gerade* levels below the $n = 2$ limit via multichannel quantum defect theory (MQDT).[20] An alternative first principles calculation of the singlet-g levels was reported by Andersson and Elander.[21] In a recent experimental study the level energies of many bound quantum states of singlet-g symmetry below the $n = 2$ dissociation limit were determined at very high precision,[22] with absolute reference to the ground state.[23,24]

To assist the discussion the calculated Born–Oppenheimer potential energy curves of all relevant states of *singlet* character and *gerade* symmetry in the region below and above the $n = 2$ limit[25–27] are displayed in Fig. 1. The $EF^1\Sigma_g^+$ and $GK^1\Sigma_g^+$ states have only bound levels below the $n = 2$ limit and exhibit a continuum above the dissociation limit. The $H\bar{H}^1\Sigma_g^+$ potential exhibits an outer well in which a series of nondissociative sharp resonances is experimentally observed.[29,30] The molecular wave functions of these states ($\bar{H}^1\Sigma_g^+$) are confined to large internuclear separations, and the large barrier prevents interaction with the levels at short internuclear separation ($H^1\Sigma_g^+$). Hence, these levels are energetically above the $n = 2$ dissociation limit,

a)Author to whom correspondence should be addressed. Electronic mail: wimu@few.vu.nl.

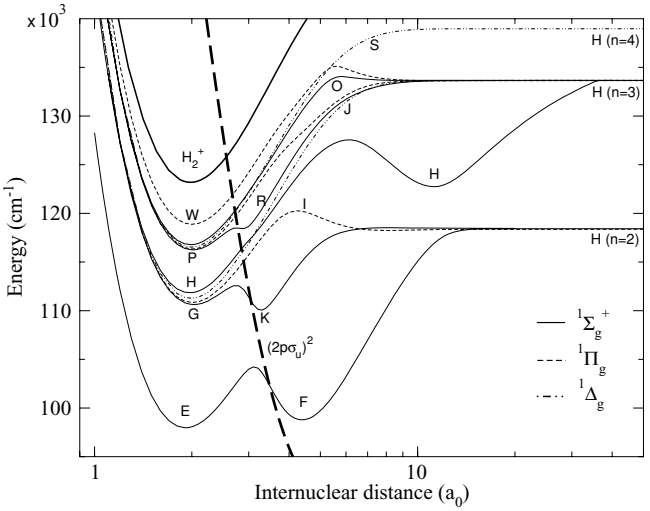

FIG. 1. Born–Oppenheimer potential energy curves of the $^1\Sigma_g^+$, $^1\Pi_g$, and $^1\Delta_g$ states near the $n = 2$ dissociation threshold of H_2 as obtained from Refs. 25–28. The dashed line represents the $(2p\sigma_u)^2$ diabatic potential causing strong dissociation in the singlet-g manifold.

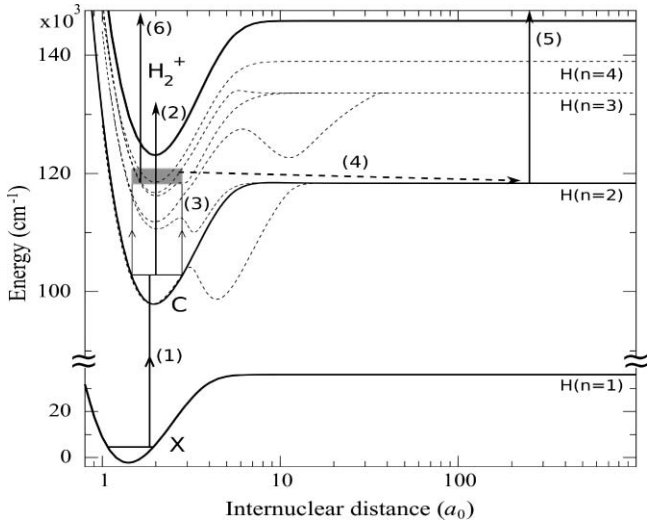

FIG. 2. The employed laser excitation scheme showing the possible channels contributing to the H^+ and H_2^+ traces. In the figure the various steps (1)–(6) as discussed in the text are indicated.

but dynamically prohibited to predissociate. Only at higher excitation energies where tunneling from the outer $(\bar{H}^1\Sigma_g^+)$ well to the inner $(H^1\Sigma_g^+)$ well occurs, these states are subject to dissociation as well as ionization.[31,32] Similarly, the levels in the shallow outer well of the $I'^1\Pi_g$ state below the $n = 2$ limit do not couple to the states confined to the $I^1\Pi_g$ inner well.[33,34]

The existence of an all-pervading repulsive potential of $(2p\sigma_u)^2$ orbital symmetry is crucial. We note that the effect of this diabatic potential, which acts as a perturber, is already included in the shape of the adiabatic curves. In effect, it causes the double-well structure of the $^1\Sigma_g^+$ adiabatic potentials. Furthermore, it is at the origin of the occurrence of strong dissociation phenomena in most singlet-g resonances in the lower energy region just above the $n = 2$ limit.

In the present laser spectroscopic study the predissociative resonances of $^1\Sigma_g^+$, $^1\Pi_g$, and $^1\Delta_g$ symmetry lying just above the $n = 2$ dissociation threshold are investigated for the first time. The assignments of the resonances, some of which tentative, are based on semiempirical spectroscopic rules.

II. EXPERIMENTAL

The present experiment entails a three-color laser excitation experiment, with photons ν_{VIS} from a tunable dye laser in the visible range (588–658 nm), UV photons ν_{UV} from an independently tunable frequency-doubled dye laser (290 nm), and extreme ultraviolet photons (≈97 nm) obtained via frequency tripling $\nu_{XUV} = 3 \times \nu_{UV}$. These induce the following multiphoton excitations and reactions in the hydrogen molecules in a collimated pulsed molecular beam expansion:

$$H_2(X^1\Sigma_g^+) + \nu_{XUV} \rightarrow H_2(C^1\Pi_u), \quad (1)$$

$$H_2(C^1\Pi_u) + \nu_{UV} \rightarrow H_2^+ + e^-, \quad (2)$$

$$H_2(C^1\Pi_u) + \nu_{VIS} \rightarrow H_2^{**}(^1\Sigma_g^+, {}^1\Pi_g, {}^1\Delta_g), \quad (3)$$

$$H_2^{**}(^1\Sigma_g^+, {}^1\Pi_g, {}^1\Delta_g) \rightarrow H(1s) + H(n = 2), \quad (4)$$

$$H(n = 2) + \nu_{UV} \rightarrow H^+ + e^-, \quad (5)$$

$$H_2^{**}(^1\Sigma_g^+, {}^1\Pi_g, {}^1\Delta_g) + \nu_{VIS} \rightarrow H_2^+ + e^-. \quad (6)$$

The excitation scheme and the relevant pathways (1)–(6) are displayed in Fig. 2. Via a 1 XUV + 1 UV two-step ionization process, following reactions (1) and (2), the XUV-laser is parked on R(0), R(1), R(2), R(3), Q(1), Q(2), and Q(3) lines in the C-X(2,0) band of H_2,[35] therewith populating specific quantum states J and (e) or (f) parity components in the $C^1\Pi_u, v = 2$ state. The generic process of the present study is the sequence (1)–(3)–(4)–(5), where a coherent 1 XUV + 1 VIS two-photon process excites a dissociative resonance (H_2^{**}), which decays to $H(1s)$ and $H(n = 2)$ fragments, with the latter converted to H^+ upon UV absorption. While probing different intermediate states and scanning the VIS-laser dissociation spectra are recorded. These signals suffer from the shot fluctuations of both the H_2 density in the pulsed molecular beam as well as of the intensity noise on the XUV-pulses generated in a nonlinear process. These fluctuations are monitored in the H_2^+ channel, which is distinguished in the experiment by time-of-flight mass selection before particle detection. The signal-to-noise ratio in the dissociation spectra (H^+ channel) is improved by dividing by the signal in the H_2^+ channel.

Figure 3 shows the traces of the generic H^+ signals, an auxiliary signal from bound states in the H_2^+ channel, and the noise-reduced dissociation channel. The auxiliary signal channel, following the route (1)–(3)–(6), results in H_2^+ detection. The excited states are longerlived nondissociative resonances occurring above the $n = 2$ limit, some of them previously observed.[19] The sharp resonance at 119 768 cm^{-1} in the H_2^+ signal channel is a typical example of a bound nondissociating level probed in the present study. It is identified as the $R^1\Pi_g^-, v = 1, J = 2$ level in H_2.

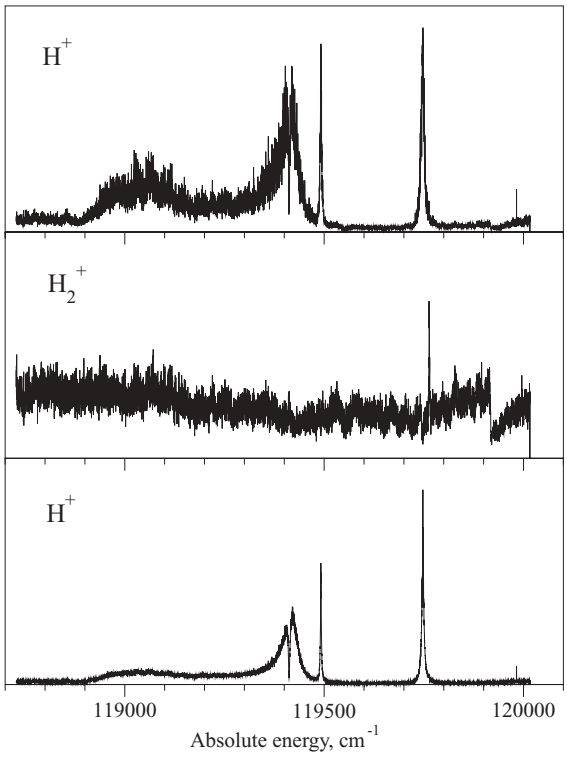

FIG. 3. Signal recording performed with multicolor laser excitation and time-of-flight mass separation. In the first step the Q(1) line in the C-X(2,0) band is excited. The upper panel shows the generic dissociation signal of the two-photon excited states of singlet-g symmetry in H^+ detection. The middle panel shows the auxiliary signal channel recorded as H_2^+. The background signal reflects the 1 XUV + 1 UV photoionization signal, which is independent of the wavelength of the additional dye laser tuned in the visible domain; the sharp resonances in the middle panel indicate bound levels of g symmetry. The lower panel is obtained by dividing the signal in the H^+ channel by that in the H_2^+ signal, thus to a large extent eliminating the noise resulting from the XUV production and fluctuations in the molecular beam density. Before this signal division takes place the H_2^+ resonances are erased from the spectrum, so that only the noise in the H_2^+ trace is remained.

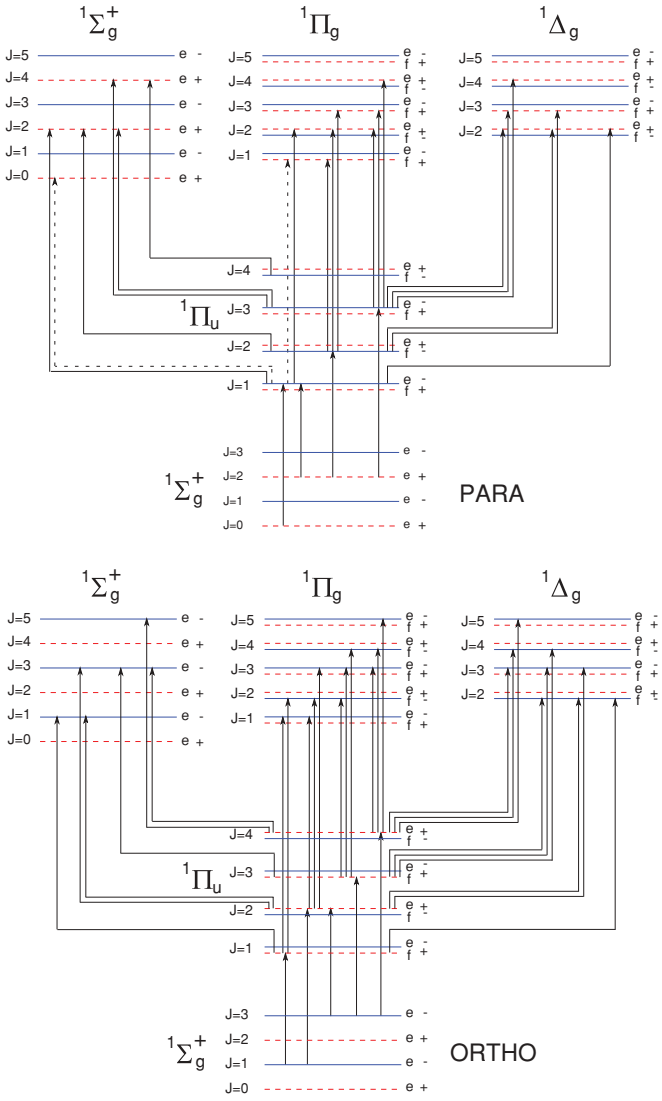

FIG. 4. Identification of possible total angular momentum states of singlet-g symmetry based on selection rules in a 1 XUV + 1 VIS double-resonance excitation scheme, for the case of para- and ortho-hydrogen. (e) and (f) indicate electronic parities and (+) and (−) indicate total parities of all states. Dashed lines represent levels with positive total parity, while solid lines represent levels with negative total parity. All allowed electric-dipole transitions are indicated. The electric-dipole selection rules for the transitions depicted with dashed lines depend on the relative orientation of the polarizations of the two photons.

III. RULES FOR ASSIGNING THE RESONANCES

For an assignment of the dissociative resonances an empirical approach is followed, which is found on a number of considerations:

(i) Due to the u–g and $\Delta\Lambda = 0, \pm 1$ dipole selection rules in optical excitation, via an intermediate state of $^1\Pi_u$ symmetry electronic states of $^1\Sigma_g^+$, $^1\Pi_g$, and $^1\Delta_g$ symmetries can be reached at the two-photon level. This holds only in so far the Hund's case (a) approximation holds, and we limit ourselves to this. States of higher electronic angular momentum may be mixed in, e.g., via configuration mixing, but these are neglected.

(ii) A distinction can be made between levels of para-hydrogen and ortho-hydrogen; optical excitation does not transfer population between these subclasses.

(iii) Selection rules impose constraints on parity, both the total (+) or (−) parity of the quantum states, and the (e) and (f) electronic symmetries.

(iv) The selection rules further impose that angular momentum quantum numbers are constrained to $\Delta J = 0, \pm 1$ transitions; this leads to a scheme displaying all allowed transitions in the coherent double-resonance experiment as shown in Fig. 4. The cases of para- and ortho-hydrogen are displayed separately.

(v) The scheme shows how for each selected intermediate state, only a limited number of final states can be reached; at the same time there exist different routes to reach each final state. In specific cases switching of the relative polarization of both laser beams alters the selection rules. One is based on the fact that for parallel polarizations the sequence $(J = 0) \rightarrow (J = 1) \rightarrow (J = 1)$ is forbidden because of a zero value for a specific Wigner-3j symbol:

$$\begin{pmatrix} 1 & 1 & 1 \\ 0 & 0 & 0 \end{pmatrix} = 0. \tag{7}$$

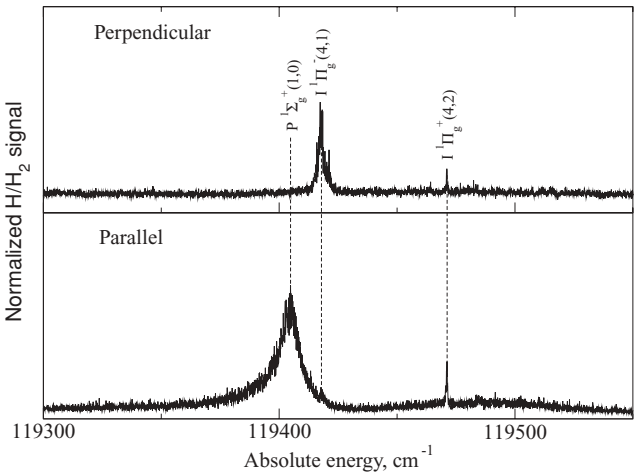

FIG. 5. Dissociation spectra obtained by 1 XUV + 1 VIS two-photon excitation via the intermediate $C^1\Pi_u$, $v = 2$, $J = 1$ state, reached via an R(0) line in the first excitation step. In the upper trace the relative orientation of the polarizations of both excitation laser beams is perpendicular, while in the lower it is parallel. With parallel polarization $J = 0$ can be excited, while with perpendicular polarization $J = 1$ is observed. The $J = 2$ level can be excited via both polarization combinations.

The other implies that a final state of $^1\Sigma_g^+$, $J = 0$ symmetry cannot be reached with perpendicular polarizations. The difference in selection rules for the different polarization geometries is used to unravel the contribution to dissociative signals of different resonances. A characteristic example is shown in Fig. 5.

(vi) Although perturbations between g symmetry states, giving rise to level shifts, are strong, rotational progressions should follow an approximate $BJ(J + 1)$ energy sequence, starting at $J = 0$ for $^1\Sigma_g^+$ states, at $J = 1$ for $^1\Pi_g$ states, and at $J = 2$ for $^1\Delta_g$ states.

(vii) By plotting the spectra on a scale of common two-photon excitation energy (as in Fig. 6) using known level energies of intermediate states[36] resonances at the same energy can be graphically identified.

(viii) As for the vibrational levels an extrapolation from the bound region can be made for those potential energy curves that support vibrational levels below $n = 2$, such as, e.g., $P^1\Sigma_g^+$ and $I^1\Pi_g$.

(ix) Guidance is obtained from the previous observation of (−) parity electronic states in emission studies[19] for the $J^1\Delta_g^-$ and $R^1\Pi_g^-$ states; these levels are not subject to predissociation. It was verified that the resonances we observed are not the ones detected in the work of Herzberg, Jungen and co-workers[11–13] in the energy region near 120 000 cm^{-1}.

(x) The Λ-doubling in the doubly degenerate $^1\Pi$ and $^1\Delta$ states should be small. It is noted that this approximation breaks down due to ℓ-uncoupling, which is in fact known to occur in the energy region just below the $n = 2$ limit.[19,20]

(xi) It is assumed that resonances of consecutive rotational quantum numbers within the same vibronic manifold exhibit approximately the same widths.

(xii) Quantum interferences in the form of dips in the spectrum (such as the one at 119 420 cm^{-1} shown in the lower panel of Fig. 6) indicate that the interacting levels have the same J quantum number.

IV. RESULTS AND DISCUSSION

In Fig. 6 typical dissociation spectra are displayed for the specific case of ortho-hydrogen for four different intermediate states probed by exciting in the first step the Q(1), R(1), Q(3), and R(3) lines in the C-X(2,0) band of H_2.

In Fig. 7 similar spectra for the case of para-hydrogen are shown, with excitation via the R(0), Q(2), and R(2) lines in the first step. The identification criteria (or "rules") mentioned in the above are used to unravel the character of the dissociative resonances. In this energy range the following excited states of g character are expected, with in brackets the molecular orbital symmetry. The $I^1\Pi_g(3d\pi_g)$ state correlates at large internuclear distance to the $n = 2$ dissociation limit. The $H^1\Sigma_g^+(3s\sigma_g)$, $P^1\Sigma_g^+(4d\sigma_g)$, $O^1\Sigma_g^+(4s\sigma_g)$, $R^1\Pi_g(4d\pi_g)$, and $J^1\Delta_g(3d\delta_g)$ correlate to the $n = 3$ dissociation limit. The $S^1\Delta_g(4d\delta_g)$ correlates to the $n = 4$ dissociation limit. The $7^1\Sigma_g^+$ state is associated with a $(5\ell_g)$ orbital and is the seventh state of $^1\Sigma_g^+$ symmetry after the ones designated as X, EF, GK, H, P, and O. Its potential energy curve was calculated by Detmer *et al.*,[28] and it exhibits, similar to the EF, GK, and $H\bar{H}$ states, a double-well structure. In the case of the $7^1\Sigma_g^+$ state the outer well is located at very large internuclear separations; in a previous three-laser excitation study it was attempted to probe bound levels at these very large intramolecular separations.[36] In the present study levels in the inner well of $7^1\Sigma_g^+$ are probed.

The assignments lead to the results listed in Table II, where next to the derived level energies also the widths of the dissociation resonances are presented. In the following the findings on each of the vibronic states are discussed. The resulting term levels are also displayed as a function of $J(J + 1)$ in Fig. 9.

A. The $I^1\Pi_g$, $v = 4$ state

As follows from Fig. 4 the states with odd J in the para-manifold and the states with even J in the ortho-manifold are states with (f) parity, hence, they must belong to a state with negative electronic symmetry, e.g., $^1\Pi_g^-$. Below the first continuum with negative symmetry emerging at around 120 300 cm^{-1}, the only rotational progression with this character that can be found in the dissociation spectra belongs to $I^1\Pi_g^-$, $v = 4$. The other states with negative symmetry do not predissociate, are observed only in the H_2^+ channel, and are in fact known from Ref. 19. The level energies of the $I^1\Pi_g^-$, $v = 4$ have been predicted in a calculation by Ross *et al.*,[18] yielding values which are remarkably close to the ones found in the present study.

Since $I^1\Pi_g^-$ is the lowest state in H_2 with negative parity (for g symmetry), predissociation by electronic or rotational coupling to another state with negative parity is excluded. Hence, the only possible mechanism through which $I^1\Pi_g^-$, $v = 4$ predissociates involves tunneling through the potential barrier of the $II'^1\Pi_g$ state. For higher J states the effective barrier is smaller, leading to enhanced tunneling rates. Indeed, this effect can be observed as an increase in linewidths for states with higher rotational quantum numbers; the

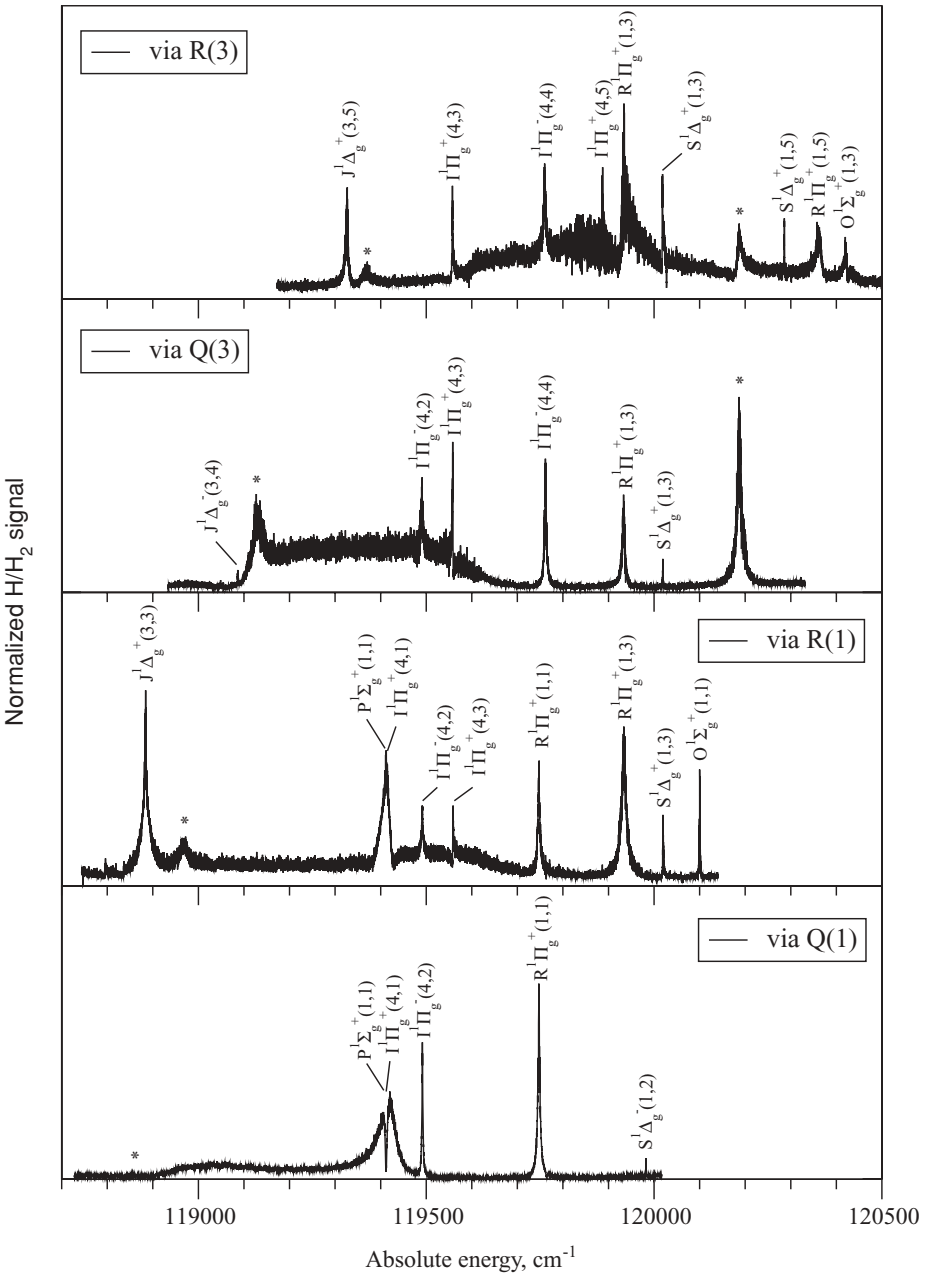

FIG. 6. Dissociation traces of ortho-hydrogen produced by 1 XUV + 1 VIS + 1 UV laser excitation. The horizontal axis represents the total term energy with respect to $X^1\Sigma_g^+$, $v = 0$, $J = 0$ reached in the two-step double-resonance excitation process.

experimental observations are displayed in detail in Fig. 8. Because this tunneling phenomenon involves only a single potential curve, the outward tunneling rates can be calculated in a semiclassical manner following the Jeffreys–Wentzel–Kramers–Brillouin (JWKB) approximation:[37]

$$\Gamma(E, J) = f_v \exp\left(-2\int\sqrt{\frac{2\mu}{\hbar}[V(R) + E_c(J) - E]}dR\right) \quad (8)$$

from which the tunneling width $\Gamma(E, J)$ can be derived for a certain energy E above the dissociation limit. The factor f_v represents the classical vibration frequency defining each tunneling event. Furthermore, μ is the reduced mass of the H_2 molecule, $V(R)$ is the *ab initio* potential energy curve for the $II'^1\Pi_g$ state[26] and $E_c(J)$ is the centrifugal energy of the molecule, which is included in the analysis. This term in the equation makes the tunneling width dependent on rotational quantum number J. As in a previous example, where the inward tunneling was calculated for the $\bar{H}^1\Sigma_g^+$ outer well state[31] the vibration frequency f_v was estimated from the vibrational spacing. This calculation leads to dissociation rates as listed in Table I.

In the work of Ross *et al.*[18] predictions were made on the lifetimes of the $I^1\Pi_g^-$, $v = 4$ levels, which were indicated as *metastable*. In a more sophisticated treatment, including the emission rate and an improved calculation of the oscillation frequency factor f_v accounting for the "softness" of the potential energy barrier with a quantum correction factor,[38] they find values (also listed in Table I) somewhat smaller than

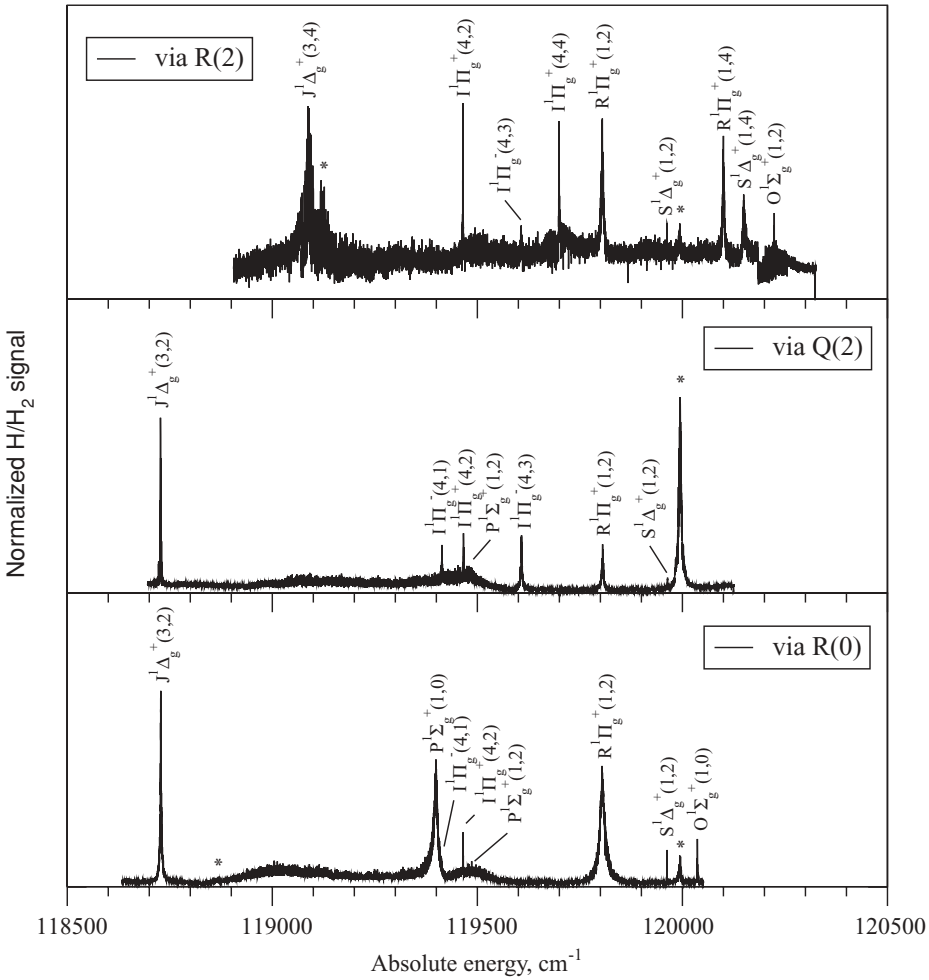

FIG. 7. Dissociation traces of para-hydrogen produced by 1 XUV + 1 VIS + 1 UV laser excitation. The horizontal axis represents the total term energy with respect to $X^1\Sigma_g^+$, $v = 0$, $J = 0$ reached in the two-step double-resonance excitation process.

from the present calculation. Remarkably, the linewidth values from experiment are larger than both calculations, a phenomenon which remains unexplained. It is conceivable that the $I^1\Pi_g^-$, $v = 4$ levels, the lowest one of (f) and g-character, exhibit an admixture of $^1\Delta_g^-$ (f); but this would reduce the linewidth instead of increasing it, since pure $^1\Delta_g^-$ states at these energies do not undergo dissociation.

Assignment of the positive symmetry states, or (e) parity states in the $I^1\Pi_g^+$, $v = 4$ manifold is based on the assumption that the Λ-doubling should not become too large. The disentanglement of the $I^1\Pi_g^+$, $v = 4$ states from the $P^1\Sigma_g^+$, $v = 1$ is based on linewidth (see below). The fact that the $^1\Pi_g^+$ levels exhibit narrower resonances than the $^1\Pi_g^-$ levels may be explained from the sign of the Λ-doubling. Levels with Π_g^+ or (e) symmetry are found to be lower in energy than levels with Π_g^- or (f) symmetry for the same angular momentum J. Therefore, the tunneling rates as calculated from Eq. (8) are expected to be smaller, in agreement with observation. In the case of the Π_g^+ states there is, however, more than one continuum available, which may cause dissociation; the direct continua pertaining to EF and GK states of Σ_g^+ symmetry interact with the Π_g^+ component and may add to dissociative decay. The fact that Π_g^+ states are found narrower indicates that the latter effect is not decisive.

The sign of the Λ-doubling in the $I^1\Pi_g$, $v = 4$ levels is counterintuitive. It is expected that the $^1\Pi_g^+$ levels are higher than the $^1\Pi_g^-$, in view of the ordering of $^1\Sigma^+$, $^1\Pi_g$, and $^1\Delta_g$ levels in an electronic manifold. Indeed, a different Λ-doublet ordering is found for lower vibrational levels in $I^1\Pi_g$. This is one of the open issues concerning our tentative assignment requiring further elucidation.

B. The $R^1\Pi_g$, $v = 1$ state

Similar to the $I^1\Pi_g$, $v = 4$ state, the long-lived emitting (f) states in $R^1\Pi_g$, $v = 1$ can be used to assign the (e) states, assuming that the Λ-doubling should not be too large. The states belonging to $R^1\Pi_g^-$, $v = 1$ are tabulated in Ref. 19 and were observed in our spectra detecting H_2^+. From the spectra, two rotational progressions of positive electronic symmetry are found in this energy range where the $R^1\Pi_g^+$ and $S^1\Delta_g^+$ are expected based on extrapolation from lower-lying levels. The progressions can be disentangled according to their linewidths. The one with narrow linewidth starts from $J = 2$

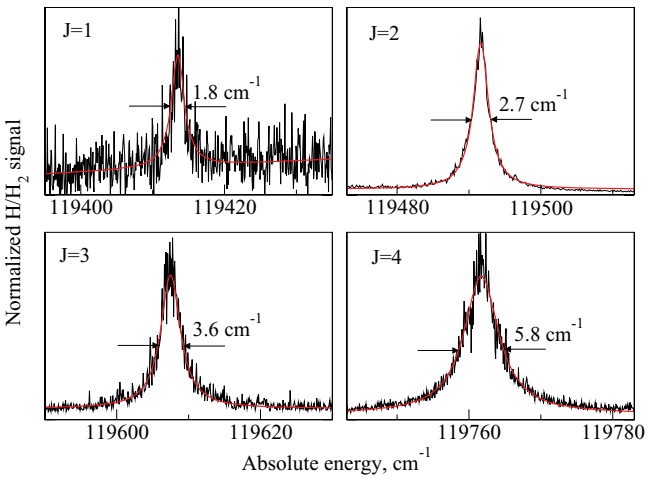

FIG. 8. Recorded spectra for transitions to rotational states belonging to $I^1\Pi_g^-$, $v = 4$. The mechanism causing their predissociation involves tunneling through the potential barrier. For higher J states the effective barrier is smaller, leading to enhanced tunneling rates, which can be observed as increasing linewidths.

TABLE I. Predissociation widths Γ of $I^1\Pi_g$, $v = 4$, J states as obtained from the experiment and from a calculating of tunnelings widths via Eq. (8). In the last column the calculated values from Ross *et al.* (Ref. 18), as converted from lifetimes, are listed. All values are in cm^{-1}.

J	$\Gamma_{obs.}$	$\Gamma_{calc.}$ (present)	$\Gamma_{calc.}$ (Ref. 18)
1	1.8	1.0	0.78
2	2.7	1.5	1.15
3	3.6	2.7	2.0
4	5.8	5.5	4.1

and is, therefore, assigned to a Δ state. The broader one, starting from $J = 1$, then belongs to $R^1\Pi_g^+$, $v = 1$. An avoided crossing between the two progressions at $J = 4$ can be observed. This results in line broadening in the progression consisting of narrow lines and in line narrowing in the progression consisting of broad lines.

C. The $P^1\Sigma_g^+$, $v = 1$ state

Assignments in this manifold are complicated due to the perturbation of the adiabatic potential energy curve by the repulsive $(2p\sigma_u)^2$ diabat, which makes the vibrational interval irregular, as is clearly visible in Fig. 1. Considering that the band origin of the $P^1\Sigma_g^+$, $v = 0$ state[17,19] is at 117 454 cm^{-1} and that a vibrational constant of about 2300 cm^{-1} is common for similar states, a $J = 0$ level is expected below 119 750 cm^{-1}. No other $^1\Sigma_g^+$ states are expected in this region and indeed a $J = 0$ state is identified at 119 405 cm^{-1} (see the lower panel of Fig. 7). The apparent 300 cm^{-1} downshift of the band origin is well explained by the outward bump of the $P^1\Sigma_g^+$ potential. The correctness of the $J = 0$ assignment is verified from its polarization properties (see Fig. 5). The linewidth of this state is relatively large, indicating that the higher J states belonging to the $P^1\Sigma_g^+$, $v = 1$ rotational manifold will also feature large linewidths. This is used to disentangle them from the narrower $I^1\Pi_g^+$, $v = 4$ resonances. Particularly interesting is the interference of both $J = 1$ rotational levels belonging to these states shown in the lower panel of Fig. 6. The rotational progression of the $P^1\Sigma_g^+$, $v = 1$ state shows a strong rotationally dependent broadening, and we speculate that levels above $J = 2$ become too broad to be assigned. Even the

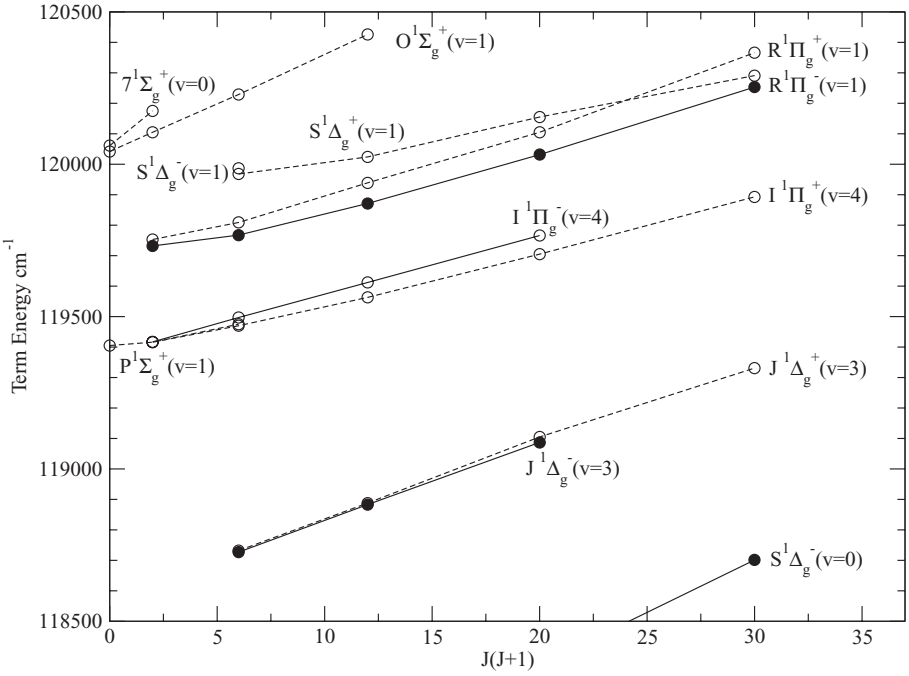

FIG. 9. Rovibronic term values as a function of $J(J + 1)$. Solid lines represent electronic states with negative rotationless parity and dashed lines with positive parity. The data points indicated with solid circles are based on emission spectroscopy (Ref. 10) and assigned by Yu and Dressler (Ref. 19). These transitions have also been observed in the present experiment detecting H_2^+. The open circles represent the term values extracted from the dissociation spectra.

TABLE II. Rovibronic term energy levels of the *gerade* states in the 118 500–120 500 cm^{-1} energy range and estimated linewidths. The accuracy of the term energy levels is 1 cm^{-1}.

State	Position	FWHM	State	Position	FWHM
$P\,^1\Sigma_g^+(v=1)$			$O\,^1\Sigma_g^+(v=1)$		
$J=0$	119 405	10.5	$J=0$	120 042	1.2
$J=1$	119 416[a]	15	$J=1$	120 105	2.2
$J=2$	119 475	50	$J=2$	120 229	1.0
			$J=3$	120 426	8
$S\,^1\Delta_g^+(v=1)$			$S\,^1\Delta_g^-(v=1)$		
$J=2$	119 968	0.3	$J=2$	119 987	<0.3
$J=3$	120 024	1.3			
$J=4$	120 155	6.6			
$J=5$	120 291	0.8			
$J\,^1\Delta_g^+(v=3)$			$J\,^1\Delta_g^-(v=3)$		
$J=2$	118 732	2.5	$J=2$		
$J=3$	118 888	14.5	$J=3$	118 888	<0.3[b]
$J=4$	119 105	20[d]	$J=4$	119 092	<0.3[b]
$J=5$	119 331	5.6			
$I\,^1\Pi_g^+(v=4)$			$I\,^1\Pi_g^-(v=4)$		
$J=1$	119 416[a]		$J=1$	119 417	1.8
$J=2$	119 470	0.8	$J=2$	119 497	2.7
$J=3$	119 563	1.5	$J=3$	119 612	3.6
$J=4$	119 705	1.2	$J=4$	119 766	5.8
$J=5$	119 893	1.9			
$R\,^1\Pi_g^+(v=1)$			$R\,^1\Pi_g^-(v=1)$		
$J=1$	119 753	5.8	$J=1$		
$J=2$	119 809	5.8	$J=2$	119 768	<0.3[b]
$J=3$	119 939	13	$J=3$	119 872	<0.3[b]
$J=4$	120 105	4.1	$J=4$	120 032	<0.3[b]
$J=5$	120 366	11			
$7\,^1\Sigma_g^+(v=0)$					
$J=0$	120 061[c]				
$J=1$	120 175[c]				

[a]These two $J=1$ levels interfere in excitation.
[b]These levels are observed in the H_2^+ signal with linewidths determined by the instrument bandwidth. They are observed also in emission spectra in Ref. 10.
[c]The uncertainty of these transitions is 5 cm^{-1}.
[d]This value is obtained from a weak and noisy part of the spectrum.

identification of the broad feature at 119 475 cm^{-1} as $J=2$ in this manifold is tentative; it might alternatively be a shape resonance of the direct continua $EF\,^1\Sigma_g^+$ or $GK\,^1\Sigma_g^+$ (see below).

D. The $O^1\Sigma_g^+$, $v=1$ state

An extrapolation similar to the one adopted before in the assignment of $P^1\Sigma_g^+$, $v=1$ predicts that the $O^1\Sigma_g^+$, $v=1$ state should lie around 120 000 cm^{-1}. Approximately at this energy we also expect the next $^1\Sigma_g^+$ state associated with one of the $(5\ell\sigma_g)$ Rydberg configurations (the $7^1\Sigma_g^+$ state). Indeed, two rotational progressions starting from $J=0$ were observed in this energy range. Both of them feature similar linewidths and, therefore, the linewidth argument cannot be used to disentangle both states. However, the rotational progressions show different rotational constants. The first progression exhibits a small rotational constant, which is derived from four observed rotational levels ($J=0-3$) and was assigned as $O^1\Sigma_g^+$, $v=1$. Extrapolation of the rotational constant for the $O^1\Sigma_g^+$, $v=0$ state ($B_0=31.2$ cm^{-1}) is in reasonable agreement with the smallest value derived from the first progression, which is therefore assigned as $O^1\Sigma_g^+$, $v=1$ ($B_1=32.0$ cm^{-1}). Certainly perturbations due to interactions with other states can affect the location of the rotational levels. Hence, due to insufficient experimental data in this region and the lack of theoretical calculations, the above assignment should be considered tentative.

E. The $7^1\Sigma_g^+$, $v=0$ state

As explained in the above, in the region around 120 000 cm^{-1} two rotational progressions starting at $J=0$ were observed. The second exhibits a higher rotational constant derived from only two observed rotational levels ($J=0,1$). The latter resonances were observed during additional measurements performed at higher excitation energy and are not included in Figs. 6 and 7. In view of the larger rotational constant, these levels were tentatively assigned to the $7^1\Sigma_g^+$, $v=0$ state. We verified that these levels do not coincide with the levels detected by Jungen *et al.*[13] in the same energy range.

F. The $S^1\Delta_g$, $v=1$ state

The (e) parity states (or positive electronic symmetry $^1\Delta_g^+$) were assigned to a progression of narrow lines (widths ~ 1 cm^{-1}) disentangling them from broader $^1\Pi_g^+$ states, as discussed in Sec. IV B. The rotational levels thus assigned to $S^1\Delta_g^+$, $v=1$ exhibit a rotational constant much smaller than in the $S^1\Delta_g$, $v=0$ state observed in emission.[19]

There is no progression of states observed which may be systematically assigned to the (f) parity states of the $S^1\Delta_g$, $v=1$ state. A narrow line was observed at 119 987 cm^{-1} in the dissociation trace recorded via the Q(1) resonance, however, without confirmation via another route; we tentatively assign this level to $S^1\Delta_g^-$, $v=1$, $J=2$. That would again imply a counterintuitive and unexplained Λ-doublet ordering for $S^1\Delta_g$, $v=1$, $J=2$.

This $^1\Delta_g^-$ level is energetically just below the barrier of the $II'\,^1\Pi_g$ potential (at 120 267 cm^{-1}), hence below the onset of the lowest continuum of negative (f) symmetry. Hence, a mechanism for predissociation must involve electronic or rotational coupling between $S^1\Delta_g^-$ and $I^1\Pi_g^-$ and tunneling through the II′ barrier. The observed width of $\Gamma=0.3$ cm^{-1}, which is limited by the instrument width, indicates that the predissociation rate is small, consistent with such a mechanism. The fact that the signal is found in the H^+ channel definitely proves that the level exhibits predissociation.

G. The $J^1\Delta_g$, $v=3$ state

Identifying this state is analogous to the procedure used with $R^1\Pi_g$, $v=1$. The long-lived (f) states are observed in the spectra detecting H_2^+. The transition frequencies obtained agree well with the data available from emission spectra,[10] with the appropriate correction of 8.00 cm^{-1} as pointed out by Yu and Dressler.[19] Note that $J^1\Delta_g^-(v=3, J=4)$ is observed

in Fig. 6 as well. We postulate that the detection channel giving rise to H^+ signal involves absorption of a third photon. This additional photon brings the system above the ionization energy, where as a result of competition between dissociation and autoionization both channels are observed simultaneously.

Knowing the (f) states, it is evident which are the (e) states as the Λ-doubling is small in Δ states. The spectral lines probing the $J^1\Delta_g^+, v = 3$ levels are among the strongest in the spectrum.

H. The $EF^1\Sigma_g^+$ and $GK^1\Sigma_g^+$ continua

In the spectra of Figs. 6 and 7 broad "bumps" appear that we assign as excitation into the dissociative continua associated with the bound $EF^1\Sigma_g^+$ and $GK^1\Sigma_g^+$ states. In another study on two-step excitation[39] it was found that the H^+ dissociation signal emerges immediately at the onset of the dissociation threshold, in that case at the $n = 3$ limit. It shows that the direct continua are important for dissociation. In the case of the $n = 2$ limit the EF and GK states provide the direct continua. Franck–Condon overlap with the EF and GK continuum wave functions may cause the background continuum excitation in the higher energy region to become structured; the fact that both the EF and GK potentials exhibit a double-well nature may cause a localization of the wave function possibly giving rise to shape resonances. Future calculations may confirm this.

I. The $H^1\Sigma_g^+$, $v = 3$ state

Considering all possible states of singlet-g symmetry in this energy region reveals that a $v = 3$ level in the inner well of the $H\bar{H}^1\Sigma_g^+$ potential is expected but not observed. Its band origin is predicted at 119 100 cm^{-1} when extrapolating from the three $v = 0 - 2$ bound levels in the $H^1\Sigma_g^+$ inner well,[22] so definitely in the observed range. The $H^1\Sigma_g^+, v = 3$ level is located well above the crossing point of the H-potential with the repulsive $(2p\sigma_u)^2$ diabatic potential. This may cause a strong (pre)dissociation, perhaps even to the extent that the resonant structure becomes washed out. If so, the $H^1\Sigma_g^+, v = 3$ resonances might contribute to the broad bumps assigned as EF and GK shape resonances in the above. In the study on the tunneling dynamics of $\bar{H}^1\Sigma_g^+$ outer well states the decay lifetime of the levels confined to the outer well were found to equal the tunneling rates.[31,32] So it was assumed that dissociation (and for the higher energy range also ionization) at short internuclear distance is immediate. If that were to be true in the lower energy region near 119 100 cm^{-1} this would explain the nonobservation of $H^1\Sigma_g^+, v = 3$ levels.

J. Further unassigned lines

There exist a few lines without assignment marked with asterisks in Figs. 6 and 7. Some of them have very low intensities and may be spurious. There are no unassigned electronic states below 119 500 cm^{-1} that could explain any of these states; this is with the exception of the $H^1\Sigma_g^+$ state, which is expected at lower energy. The transition marked on the dissociation trace via R(1) is not reproducible, which indicates that it can be an artifact. We speculate that these features relate to higher-lying dissociative resonances probed via multiphoton excitation from the intermediate $C^1\Pi_u, v = 2$ levels.

In addition strong lines were observed at 119 999 cm^{-1} with identified $J = 2$ rotational quantum number, and at 120 192 cm^{-1} with possibilities $J = 3$ or 4. These unassigned lines at the high-energy edge of the presently covered spectral window might be the start of higher lying rotational progressions, e.g., of the 5ℓ manifold.

V. CONCLUSION AND OUTLOOK

In the present experimental investigation on coherent two-step excitation the level structure of dissociating resonances in the singlet-g compartment of H_2 just above the $n = 2$ threshold have been recorded for the first time. Based on spectroscopic rules the resonances are assigned in terms of $^1\Sigma_g^+$, $^1\Pi_g$, and $^1\Delta_g$ electronic symmetries as well as rovibrational quantum numbers. These assignments are tentative in several cases because perturbations will affect the level structure above $n = 2$, as it occurs below the $n = 2$ limit.

In the present study 1 XUV + 1 VIS excitation leads to dissociation of the H_2 molecule. Experimentally the $H(n = 2)$ fragments are detected without distinguishing between $2s$ and $2p$ atomic hydrogen products. In principle a more sophisticated experimental approach is feasible, whereby only $2s$ products are probed. By employing a third independent pulsed laser system at delays exceeding 20 ns with respect to the two first excitation lasers the $2p$ fragments will not be detected in view of their short lifetime (~1 ns). Through the use of varying delays the contribution of $2s$ and $2p$ fragments may be disentangled, providing more detailed information on the dissociation phenomena and the symmetries of the states involved.

Perturbations in the level structure above the $n = 2$ limit, where dissociation continua are expected to play a decisive role, can be dealt with in the theoretical framework of MQDT, which has proven successful in describing the level structure and the dissociation as well as ionization dynamics of molecules. In particular, for the H_2 molecule MQDT calculations are performed based on first principles without empirical parameters. MQDT has thus provided successful explanation of the level structure and dissociation dynamics in the singlet-u compartment,[40] and later also for the *triplet* states both of g and u character.[41,42]

In the singlet-g compartment the observations on the decay of highly excited resonances above the ionization potential[43] were explained in the framework of MQDT.[44] The dissociation range just above the $n = 2$ limit poses the problem of correctly incorporating the effect of the repulsive $(2p\sigma_u)^2$ potential extending to large internuclear separation. The present observations on the dissociative resonances above $n = 2$ may guide future theoretical work in this range.

ACKNOWLEDGMENTS

The authors wish to thank Dr. E. Reinhold for fruitful discussions and for assistance in the calculation of the tunneling

widths in the $II'^1\Pi_g$ potential, and two anonymous referees for useful remarks that helped improve the manuscript.

[1]W. Lichten, Phys. Rev. **120**, 848 (1960).
[2]E. E. Eyler and F. M. Pipkin, Phys. Rev. A **27**, 2462 (1983).
[3]N. Bjerre, S. Keiding, L. J. Lembo, and H. Helm, Phys. Rev. Lett. **60**, 2465 (1988).
[4]L. D. A. Siebbeles, J. M. Schins, J. Los, and M. Glass-Maujean, Phys. Rev. A **44**, 1584 (1991).
[5]T. A. Miller and R. S. Freund, J. Chem. Phys. **61**, 2160 (1974).
[6]E. Reinhold, R. Buning, U. Hollenstein, A. Ivanchik, P. Petitjean, and W. Ubachs, Phys. Rev. Lett. **96**, 151101 (2006).
[7]W. Ubachs, R. Buning, K. S. E. Eikema, E. Reinhold, J. Mol. Spectrosc. **241**, 241 (2007).
[8]M. Glass-Maujean, J. Breton, and P. M. Guyon, Chem. Phys. Lett. **63**, 591 (1979).
[9]G. D. Dickenson, T. I. Ivanov, M. Roudjane, N. de Oliveira, D. Joyeux, L. Nahon, W.-Ü. L. Tchang-Brillet, M. Glass-Maujean, I. Haar, A. Ehresmann, and W. Ubachs, J. Chem. Phys. **133**, 144317 (2010).
[10]H. M. Crosswhite, *The hydrogen molecule wavelength tables of Gerhard Heinrich Dieke* (Wiley-Interscience, 1972).
[11]G. Herzberg and C. Jungen, J. Chem. Phys. **77**, 5876 (1982).
[12]C. Jungen, I. Dabrowski, G. Herzberg, and D. J. W. Kendall, J. Chem. Phys. **91**, 3926 (1989).
[13]C. Jungen, I. Dabrowski, G. Herzberg, and M. Vervloet, J. Chem. Phys. **93**, 2289 (1990).
[14]D. J. Kligler and C. K. Rhodes, Phys. Rev. Lett. **40**, 309 (1978).
[15]E. E. Marinero, C. T. Rettner, and R. N. Zare, Phys. Rev. Lett. **48**, 1323 (1982).
[16]K. Tsukiyama, J. Ishii, and T. Kasuya, J. Chem. Phys. **97**, 875 (1992).
[17]H. Aita, Y. Ogi, and K. Tsukiyama, J. Mol. Spectr. **232**, 315 (2005).
[18]S. C. Ross, M. Fijii, J. Ando, and K. Tsukiyama, Mol. Phys. **105**, 1643 (2007).
[19]S. Yu and K. Dressler, J. Chem. Phys. **101**, 7692 (1994).
[20]S. C. Ross and Ch. Jungen, Phys. Rev. A **50**, 4618 (1994).
[21]S. Andersson and N. Elander, Phys. Rev. A **69**, 052507 (2004).
[22]D. Bailly, E. J. Salumbides, M. Vervloet, and W. Ubachs, Mol. Phys. **108**, 827 (2010).
[23]S. Hannemann, E. J. Salumbides, S. Witte, R. Zinkstok, E.-J. van Duijn, K. S. E. Eikema, and W. Ubachs, Phys. Rev. A **74**, 062514 (2006).
[24]E. J. Salumbides, D. Bailly, A. Khramov, A. L. Wolf, K. S. E. Eikema, M. Vervloet, and W. Ubachs, Phys. Rev. Lett. **101**, 223001 (2008).
[25]L. Wolniewicz and K. Dressler, J. Chem. Phys. **100**, 444 (1994).
[26]L. Wolniewicz, J. Mol. Spectrosc. **169**, 329 (1995).
[27]L. Wolniewicz, J. Mol. Spectrosc. **174**, 132 (1995).
[28]T. Detmer, P. Schmelcher, and L. S. Cederbaum, J. Chem. Phys. **109**, 9694 (1998).
[29]E. Reinhold, W. Hogervorst, and W. Ubachs, Phys. Rev. Lett. **78**, 2543 (1997).
[30]E. Reinhold, W. Hogervorst, W. Ubachs, and L. Wolniewicz, Phys. Rev. A **60**, 1258 (1999).
[31]E. Reinhold, W. Hogervorst, and W. Ubachs, J. Chem. Phys. **112**, 10754 (2000).
[32]S. C. Ross, T. Toshinari, Y. Ogi, and K. Tsukiyama, J. Chem. Phys. **125**, 133205 (2006).
[33]E. Reinhold, A. de Lange, W. Hogervorst, and W. Ubachs, J. Chem. Phys. **109**, 9772 (1998).
[34]S. C. Ross, J. Ando, and K. Tsukiyama, Mol. Phys. **108**, 109 (2010).
[35]P. C. Hinnen, W. Hogervorst, S. Stolte, and W. Ubachs, Can. J. Phys. **72**, 1032 (1994).
[36]J. C. J. Koelemeij, A. de Lange, W. Ubachs, Chem. Phys. **287**, 349 (2003).
[37]P. Senn and K. Dressler, J. Chem. Phys. **87**, 1205 (1987).
[38]J. N. L. Connor and A. D. Smith, Mol. Phys. **43**, 397 (1981).
[39]C. R. Scheper, C. A. de Lange, E. Reinhold, A. de Lange, and W. Ubachs, Chem. Phys. Lett. **312**, 131 (1999).
[40]C. Jungen and O. Atabek, J. Chem. Phys. **66**, 5584 (1977).
[41]A. Matzkin, C. Jungen, and S. C. Ross, Phys. Rev. A **62**, 062511 (2000).
[42]S. C. Ross, C. Jungen, and A. Matzkin, Can. J. Phys. **79**, 561 (2001).
[43]H. Rottke and K. H. Welge, J. Chem. Phys. **97**, 908 (1992).
[44]C. Jungen and S. C. Ross, Phys. Rev. A **55**, R2503 (1997).